Electric-field-induced phase transitions of $(1-x)PbMg_{1/3}Nb_{2/3}O_3-xPbTiO_3$ crystals studied by optical methods

2009 J. Phys.: Condens. Matter 21 335902

(http://iopscience.iop.org/0953-8984/21/33/335902)

J. Phys.: Condens. Matter **21** (2009) 335902 (6pp) doi:10.1088/0953-8984/21/33/335902

Electric-field-induced phase transitions of $(1-x)PbMg_{1/3}Nb_{2/3}O_3$–$xPbTiO_3$ crystals studied by optical methods

Xiaobing Li[1,2,3], Feifei Wang[1,2], Yanting Lin[1,2], Linhua Liu[1,2], Xiangyong Zhao[1], Haosu Luo[1] and Di Lin[1]

[1] State Key Laboratory of High Performance Ceramics and Superfine Microstructure, Shanghai Institute of Ceramics, Chinese Academy of Science, Shanghai 200050, People's Republic of China
[2] Graduate University of the Chinese Academy of Sciences, Beijing 100049, People's Republic of China

E-mail: lxbing@mail.sic.ac.cn

Received 28 February 2009, in final form 12 July 2009
Published 28 July 2009
Online at stacks.iop.org/JPhysCM/21/335902

Abstract

The phase transitions of as-grown $(1-x)PbMg_{1/3}Nb_{2/3}O_3$–$xPbTiO_3$ (PMN–xPT) crystals with PT compositions of $x = 0.31$ and 0.38 under a dc electric field were observed in a polarization microscope. The optical transmissions of the crystals under dc electric fields were measured in the wavelength region around their optical absorption edges. The band gaps of the orthorhombic and tetragonal phases under the applied electric field were obtained. By combining both of the optical methods, the phase transition from the tetragonal to the orthorhombic phase was observed in PMN–0.38PT crystals when the electric field along the $[110]_{cub}$ direction reaches up to 300 V mm^{-1}. Whereas the PMN–0.31PT crystals undergo the pseudo-phase-transition under a dc electric field along the $[110]_{cub}$ direction. The pseudo-phase-transition possibly stems from the reorientation and growth of microdomains in PMN–0.31PT crystals.

(Some figures in this article are in colour only in the electronic version)

1. Introduction

Relaxor-based perovskite ferroelectrics, such as $(1-x)PbMg_{1/3}Nb_{2/3}O_3$–$xPbTiO_3$ (PMN–xPT) and $(1-x)PbZn_{1/3}Nb_{2/3}O_3$–$xPbTiO_3$ (PZN–xPT), show outstanding electromechanical properties near the morphotropic phase boundary (MPB), which separates the rhombohedral (R) and tetragonal (T) phases [1, 2]. The origin of the high piezoelectric response near the MPB and the intrinsic structure for relaxation have been the subjects of discussion for many years, and many theories have been proposed [3–14]. The real breakthrough came out of the microstructure study of $Pb(Zr_{1-x}Ti_x)O_3$ by Noheda *et al* [15–18], which showed a monoclinic phase within a narrow region, $0.45 < x < 0.52$, around the MPB. Then, the corresponding polarization rotation mechanism was proposed based on the first principles studies of a $BaTiO_3$ single crystal at zero temperature [8]. Furthermore, eighth-order free-energy expansion was also carried out to prove the existence of the monoclinic phase [19]. Therefore, the monoclinic phase is believed to be the intermediate phase between R and T, and the intermediate monoclinic or orthorhombic phases are believed to be involved in the phase transition from the R to T phase under electric fields [20, 21].

However, adaptive ferroelectric phase theory questioned the existence of the monoclinic phase in these materials [9, 22]. They stated that the lattice parameters of the monoclinic phase calculated from Rietveld refinements are directly dependent on those of the tetragonal and cubic parent phases. The monoclinic one is just an average over the miniaturized tetragonal nanodomains, which reach up to tens of nanometers without being able to diffract incoherently. Both the miniaturization and low domain-wall energy can enhance the piezoelectric properties of the material, as the domains are more easily reoriented. Moreover, experiments in a high-resolution transmission electron microscope (TEM) and X-band EPR spectra [23, 24] show that the hierarchical domain structure is a self-assembly of nanodomains with tetragonal

[3] Author to whom any correspondence should be addressed.

structure. Their submicrodomains appear as a tetragonal phase, but macrodomains exhibit the monoclinic state due to an averaging effect. Another important model proposed by Glazer *et al* [25], suggested that changes in the range of structural order play the most important role in the enhanced properties around the MPB.

In the present work, we report experimental results, which indicate the electric-field-induced real phase transition in the crystals far away from the MPB and the pseudo-phase-transition in the crystals near the MPB. These results were obtained by combining the simultaneous observation of the domains in an optical polarization microscope and optical absorption edge measurements.

2. Experimental details

Large size and high quality PMN–xPT single crystals were grown directly from melt by the modified Bridgman technique [26, 27]. The Curie temperatures (T_C) of the as-grown crystals were measured to determine the compositions of the samples. The selected samples with $x = 0.38$ and 0.31 were oriented and cut perpendicular to the $[001]_{cub}$ and $[110]_{cub}$ directions as confirmed by x-ray diffractometer. The two samples were polished down to the thickness of 0.1 mm along the $[001]_{cub}$ and $[110]_{cub}$ directions, respectively, by alumina and diamond compounds (with decreasing average grit size down to 0.5 μm) for the domain observations. Electrodes with silver paste were prepared on their corresponding transverse $(110)_{cub}$ and $(\bar{1}10)_{cub}$ faces, and they were then sintered at 750 °C (30 min) for the measurements under a dc electric field.

An optical polarization microscope (Olympus U-CMAD3, Japan) set with a 0°/90° crossed polarizer analyzer was used to study the domains structures in the samples. The possible optical extinctions crossing $[001]_{cub}$ were observed when the dc electric field was applied in the crystal along the $[110]_{cub}$ direction, and also the extinctions crossing $[110]_{cub}$ were obtained when applying the dc electric field along the $[\bar{1}10]_{cub}$ direction.

The transmission spectra were measured with the incident light along the $[001]_{cub}$ direction, and the dc electric fields (i.e. 30, 100, 300, 500, 700 and 900 V mm^{-1}) were simultaneously applied in the samples along the $[110]_{cub}$ direction for about 10 min. The corresponding transmission spectra were obtained in the wavelength range from 380 to 470 nm using a spectrophotometer (Shimadzu UV-2501PC, the worst case index accuracy is ±0.1%) at room temperature.

3. Results and discussions

3.1. The phase transitions under an electric field observed by an optical polarization microscope

The optical extinction directions of different domains can be identified by the birefringence contrast created with a compensator applied in appropriate directions, thereby the domain structures and the phase symmetry have been analyzed [28–35]. As shown in figure 1, the domains of as-grown PMN–0.38PT crystals were observed in an optical polarization microscope, and the phase transition was studied in real time by applying the electric field along the $[110]_{cub}$ direction.

For the PMN–0.38PT crystals which are far away from the MPB, the optical extinction crossing $[001]_{cub}$ at the angle of 0° (see figure 1(a)) is evidence of their tetragonal phase at room temperature. Under a dc electric field along the $[110]_{cub}$ direction, the optical extinction crossing $[001]_{cub}$ at an angle of 0° disappears when the electric field is larger than 300 V mm^{-1} (see figure 1(b)). While for the observation crossing $[001]_{cub}$ at an angle of 45° (see figures 1(c) and (d)), the optical extinction appears when the electric field is applied in the $[110]_{cub}$ direction (see figure 1(d)). Combined with the observation crossing $[110]_{cub}$ of the PMN–0.38PT crystal with an electric field along the $[\bar{1}10]_{cub}$ direction, it can be confirmed that the orthorhombic phase is induced in the PMN–0.38PT crystal by a dc field at 300 V mm^{-1}, and after removing the electric field it will return to the tetragonal phase.

While for the PMN–0.31PT crystal, shown in figure 2(a), the optical extinction crossing $[001]_{cub}$ at an angle of 15° indicates a monoclinic phase. When the applied electric field is larger than 350 V mm^{-1} along the $[110]_{cub}$ direction the optical extinction disappeared (see figure 2(b)). Thus, a transition from the monoclinic phase to other phases occurred, and the crystal did not return to the monoclinic phase when the electric field was removed. The new phase shows optical extinction crossing $[001]_{cub}$ at an angle of 45°, which is probably rhombohedral or orthorhombic or another monoclinic phase. Moreover, to confirm the symmetry, the observation crossing $[110]_{cub}$ was carried out by applying an electric field in the $[\bar{1}10]_{cub}$ direction (see figures 2(c) and (d)). The domains shows optical extinction at an angle of 0° (see figure 2(c)) with respect to the $[\bar{1}10]_{cub}$ direction, which indicates the orthorhombic phase when combined with the observation along the $[001]_{cub}$ direction. Therefore, the crystal will undergoes a phase transition from the monoclinic to orthorhombic phase when a threshold electric field of 350 V mm^{-1} is applied along the $[\bar{1}10]_{cub}$ direction, as shown in figure 2.

The polarized light is sensitive to the symmetry of the crystal structure, but the spatial resolution of the optical polarization microscopy is low. Therefore, the observed symmetry of macrodomains may be different from that of microstructures. Therefore the shifts of band gaps under an electric field were measured to confirm the phase transitions.

3.2. Optical absorption near the fundamental absorption edge under an electric field

The optical absorption edge is caused by the onset of optical transitions across the fundamental band gap of the material. This naturally leads us to investigate the physical processes that occur when electrons are excited between the bands of a solid by making optical transitions [36]. The energy band structure is determined by the lattice of the crystals, so the phase transition, which means the mutation of the crystal lattices, under an electric field will cause an abrupt change of the energy band, including a change of the band gaps. The band

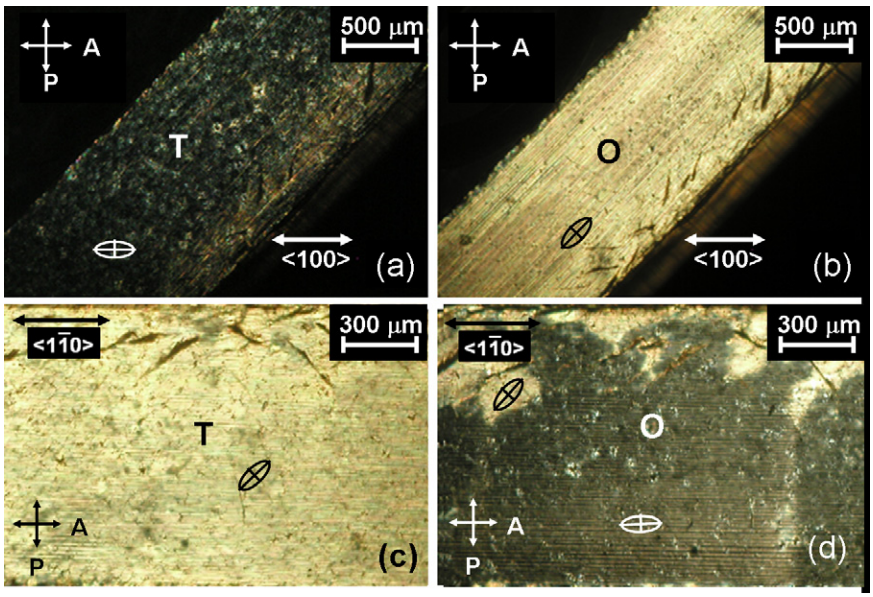

Figure 1. PMN–0.38PT crystals in the optical polarization microscope, (a) extinction crossing $[001]_{cub}$, (b) domains under an electric field of 300 V mm^{-1} along the $[110]_{cub}$ direction, (c) observation crossing $[001]_{cub}$, (d) extinction crossing $[001]_{cub}$ under an electric field of 900 V mm^{-1} along the $[110]_{cub}$ direction.

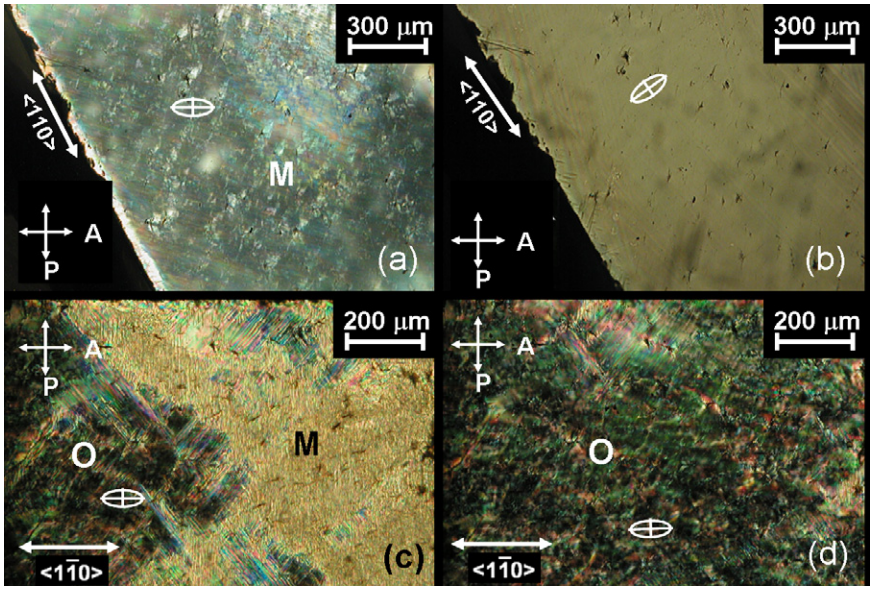

Figure 2. PMN–0.31PT crystals in an optical polarization microscope, (a) extinction crossing $[001]_{cub}$, (b) domains under an electric field of 500 V mm^{-1} along the $[110]_{cub}$ direction, (c) extinction crossing $[110]_{cub}$ under an electric field of 350 V mm^{-1} along the $[110]_{cub}$ direction, (d) the extinction crossing $[110]_{cub}$ under an electric field of 900 V mm^{-1} along the $[1\bar{1}0]$ direction.

gaps of the crystals could be obtained from the transmission spectra measurements, therefore, the phase transition under an electric field could be studied by the changes of transmission spectra.

When a crystal is irradiated, some photons will be reflected, absorbed, or scattered and others transmitted. The transmission (T) at a given wavelength can be calculated by using the Mclean formula [36]

$$T = \frac{(1-R)^2 \exp(-\alpha d)}{1 - R^2 \exp(-2\alpha d)}, \tag{1}$$

where α is the absorption coefficient, d is the thickness of the sample, and R is the reflectance of the two faces of the sample, which can be calculated by the Fresnel expression [36]

$$R = (n-1)^2/(n+1)^2, \tag{2}$$

where n is the index of refraction at a given wavelength. The wavelength dependence of the refractive index (n_o) of the PMN–0.38PT crystal can be obtained from the modified Sellmeier equation [37, 38]

$$n_o^2(\lambda) = 6.2144 + \frac{0.2151}{\lambda^2 - 0.0686} - 0.0004\lambda^2. \tag{3}$$

The optical wavelength (λ) dependences of transmittance (T) from 380 to 430 nm were measured experimental. In such a way the optical wavelength dependence of absorption coefficient α could be obtained by combining the measured $T(\lambda)$ with formulae (1)–(3). Furthermore, the direct band gaps of crystals could be deduced from the absorption coefficient α and the energy of the incident light $h\nu$ by using the Tauc equation [39]

$$(\alpha h\nu)^2 = B(h\nu - E_g), \tag{4}$$

where h is the Planck constant, $\nu = 2\pi/\lambda$ is the wavevector, B is a constant, and E_g is the band gap of the crystal. Therefore, E_g could be obtained from the transmission spectra, and the change of the energy band of the crystals under electric field could be observed. Figure 3(a) shows the $T(\lambda)$ of PMN–0.38PT crystal with incidence along the [001] direction, meanwhile, the electric field is applied along the $[110]_{cub}$ direction up to 900 V mm^{-1}. It is obvious that the curves could be classified into two groups. The calculated band gaps of the PMN–0.38PT crystal are obtained from the measurements of transmittance and formulae (1)–(4), which are shown in figure 3(b). In the process of gradually applying electric fields in the PMN–0.38PT crystal, two band gaps, 3.074 ± 0.1% and 3.096 ± 0.1% eV, are obtained, corresponding to the tetragonal and orthorhombic phases respectively. The threshold electric field for this phase transition is 300 V mm^{-1}. In this aspect, a real phase transition has happened, because the band gap change is directly related to a change of lattice.

Using the same method, the phase transition of the PMN–0.31PT crystal near MPB was also studied under an electric field. The wavelength dependences of transmittance in different electric fields were measured and are shown in figure 4(a). The refractive index dependence of wavelength of the PMN–0.31PT crystal could be obtained from the modified Sellmeier equation [40]

$$n^2(\lambda) = 6.6344 + \frac{0.088}{\lambda^2 - 0.0979} - 0.6123\lambda^2. \tag{5}$$

Also, the band gaps of the PMN–0.31PT crystal are obtained by combining the measurement of transmittance and formulae (1)–(4), seen in figure 4(b). It is shown that the band gaps (3.117 ± 0.1% eV) of the crystals did not change under an electric field up to 900 V mm^{-1}. This means that the lattices of the crystals are the same in the whole electric field range, as the band gap of the crystal is determined by the lattice. However, this is different from the as-proposed result obtained from an optical polarization microscope in the PMN–0.31PT crystal, where two phases were observed under different electric fields. It indicates that a pseudo-phase-transition was induced in PMN–0.31PT crystals by an electric field in this experiment.

3.3. The phase transition under electric field

For the PMN–xPT crystals, the extent of long range order decreases with the reduction of PT composition (x) and is followed by a subsequent decrease in the size of domains. When the composition is near the MPB, nanodomains are believed to form in these ferroelectric solid

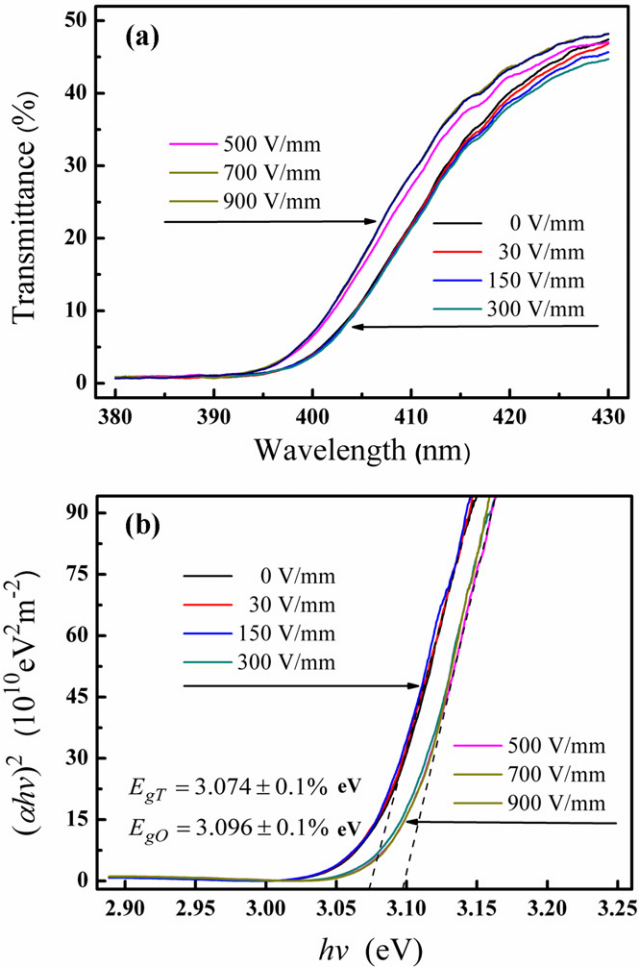

Figure 3. Transmittance spectra (a) and the $(\alpha h\nu)^2$ versus $h\nu$ plot (b) of PMN–0.38PT single crystals.

solutions [9, 23, 41]. The macrodomains observed in optical polarization microscopy are the average of the microdomains, and the symmetry of the macrodomains is determined by the volume ratio of microdomains with different orientations. In PMN–0.31PT crystals, there is no phase transition observed by band gaps measurements, even when an electric field of 900 V mm^{-1} is applied in the crystals. It indicates that the electric field is along the spontaneous direction of the domains, which is the $[110]_{cub}$ direction for the orthorhombic phase [20]. Moreover, the phase transition observed in optical polarization microscopy under the threshold electric field of 350 V mm^{-1} might be the reorientation of orthorhombic microdomains. The different volume ratio of the orthorhombic domains creates the monoclinic symmetry on the macro-scale. Furthermore, a vertical line was found in the E–T phase diagrams, which is connected to the appearance of a macroscopic state, and the state is due to the onset of freezing of large PNR's [14]. Meanwhile, the electric field could cause the gradual coalescence of polar nanoregions and the successive abrupt formation of large ferroelectric domains [42]. Therefore, under an electric field, the microdomains could abruptly grow large enough to prevent the averaging effect, and then the domains will exhibit their

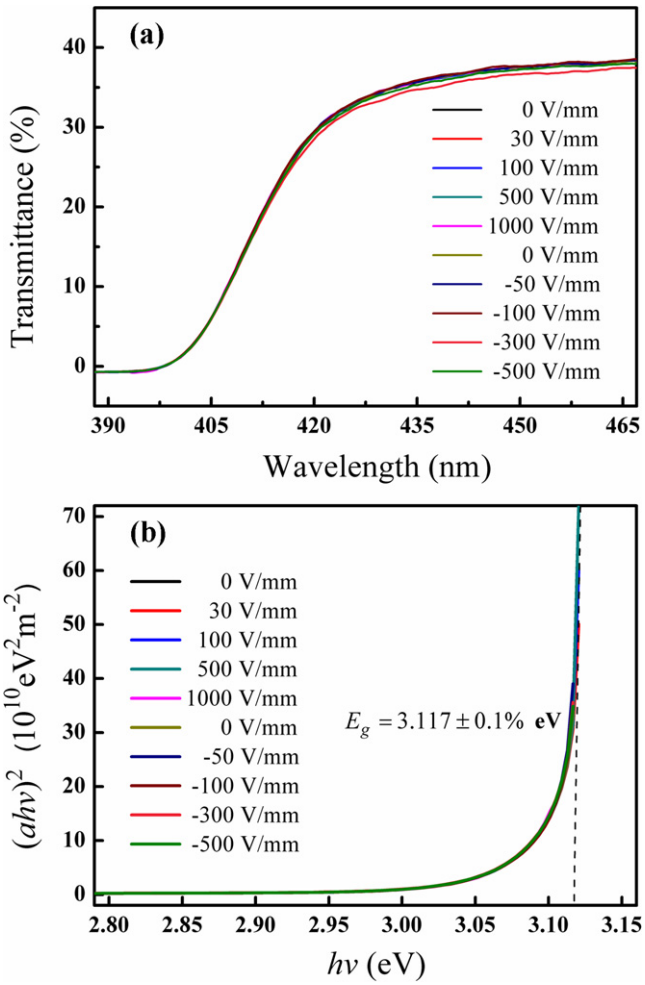

Figure 4. Transmittance spectra (a) and the $(\alpha h\nu)^2$ versus $h\nu$ plot (b) of PMN–0.31PT single crystals.

intrinsic orthorhombic phase. Based on the above analysis, in the PMN–0.31PT crystals, the monoclinic phase is composed of orthorhombic microdomains while in the macroscopic scale it appear as monoclinic due to an averaging effect. There is no averaging effect in the PMN–0.38PT crystals composed essentially of macrodomains.

4. Conclusion

The phase transition from the tetragonal to orthorhombic phase in the PMN–0.38PT crystal is confirmed by the polarization microscope and optical absorption edge methods under an electric field. The band gaps of the tetragonal and orthorhombic phase are 3.074 ± 0.1% and 3.096 ± 0.1% eV, respectively. However, for the PMN–0.31PT crystal, the results obtained by the two methods are not consistent. Monoclinic and orthorhombic phases are observed in the polarization microscope, but only one phase was obtained by optical transmittance measurements. This can be understood from the averaging effect of orthorhombic microdomains for compositions falling into the MPB region. The phase transition from the monoclinic to the orthorhombic phase is a kind of pseudo-phase-transition, which is actually the reorientation and growth of orthorhombic microdomains.

Acknowledgments

This work was financially supported by the 863 High Technology and Development Project of the People's Republic of China (Grant No. 2008AA03Z410), the Natural Science Foundation of China (Grant Nos 60837003, 50777065 and 50602047), Shanghai Municipal Government (08JC1420500), the Innovation Fund of the Shanghai Institute of Ceramics (O99ZC4140G), and the Fund of the National Engineering Research Center for Optoelectronic Crystalline Materials (2005DC105003) with Grant No. 2007K05.

References

[1] Kuwata J, Uchino K and Nomura S 1981 *Ferroelectrics* **37** 579
[2] Shrout T R, Chang Z P, Kim N and Markgraf S 1990 *Ferroelectr. Lett. Sect.* **12** 63
[3] Carl K and Härdtl K H 1971 *Phys. Status Solidi* a **8** 87
[4] Shirobokov M Y and Khodolenko L P 1951 *Zh. Eksp. Teor. Fiz.* **21** 1239
[5] Benguigui L 1972 *Solid State Commun.* **11** 825
[6] Wersing W 1974 *Ferroelectrics* **7** 163
[7] Pinczuk A 1973 *Solid State Commun.* **12** 1035
[8] Fu H X and Cohen R E 2000 *Nature* **403** 281
[9] Jin Y M, Wang Y U, Khachaturyan A G, Li J F and Viehland D 2003 *Phys. Rev. Lett.* **91** 197601
[10] Kutnjak Z, Petzelt J and Blinc R 2006 *Nature* **441** 956
[11] Xu G Y, Zhong Z, Bing Y, Ye Z G and Shirane G 2006 *Nat. Mater.* **5** 134
[12] Vugmeister B E and Rabitz H 2001 *Phys. Rev.* B **65** 024111
[13] Pirc R, Blinc R and Kutnjak Z 2002 *Phys. Rev.* B **65** 214101
[14] Raevski I P, Prosandeev S A, Emelyanov A S, Raevskaya S I, Colla E V, Viehland D, Kleemann W, Vakhrushev S B, Dellis J L, Marssi M E and Jastrabik L 2005 *Phys. Rev.* B **72** 184104
[15] Noheda B, Cox D E, Shirane G, Gonzalo J A, Cross L E and Park S E 1999 *Appl. Phys. Lett.* **74** 2059
[16] Noheda B, Cox D E and Shirane G 1999 *Appl. Phys. Lett.* **74** 2059
[17] Noheda B, Cox D E, Shirane G, Guo R, Jones B and Cross L E 2000 *Phys. Rev.* B **63** 014103
[18] Guo R, Cross L E, Park S E, Noheda B, Cox D E and Shirane G 2000 *Phys. Rev. Lett.* **84** 5423
[19] Vanderbilt D and Cohen M H 2001 *Phys. Rev.* B **74** 2059
[20] Li Z R, Xu Z, Yao X and Cheng Z Y 2008 *J. Appl. Phys.* **104** 024112
[21] Li Z R, Xu Z, Xi Z Z, Wei X Y and Yao X 2003 *Opt. Mater.* **23** 429
[22] Jin Y M, Wang Y U, Khachaturyan A G, Li J F and Viehland D 2003 *J. Appl. Phys.* **94** 3629
[23] Wang H, Zhu J, Lu N, Bokov A A, Ye Z G and Zhang X W 2006 *Appl. Phys. Lett.* **89** 042908
[24] Schönau K A, Schmitt L A, Knapp M, Fuess H, Eichel R-A, Kungl H and Hoffmann M J 2007 *Phys. Rev.* B **75** 184117
[25] Glazer A M, Thomas P A, Baba-Kishi K Z, Pang G K H and Tai C W 2004 *Phys. Rev.* B **70** 184123
[26] Luo H, Xu G, Xu H, Wang P and Yin Z 2000 *Japan. J. Appl. Phys.* **39** 5581
[27] Wan X, Wang J, Chan H L W, Choy C L, Luo H and Yin Z 2004 *J. Cryst. Growth* **263** 251
[28] Wahlstrom E 1979 *Optical Crystallography* (New York: Wiley)

[29] Schmid H, Setter N and Cola E L 1991 *Ferroelectric Ceramics* (Basel: Birkhauser)
[30] Tu C S, Chien R R, Hung C M, Schmidt V H, Wang F T and Tseng C T 2007 *Phys. Rev.* B **75** 212101
[31] Ye Z G and Dong M 1999 *J. Appl. Phys.* **87** 2312
[32] Chien R R, Hugo S V, Tu C S, Hung L W and Luo H 2004 *Phys. Rev.* B **69** 172101
[33] Tu C S, Wang F T, Hung C M, Chien R R and Luo H 2006 *J. Appl. Phys.* **100** 104104
[34] Bao P, Yan F, Lu X M, Zhu J S, Shen H M, Wang Y N and Luo H S 2006 *Appl. Phys. Lett.* **88** 092905
[35] Xu G S, Luo H S, Xu H Q and Yin Z W 2001 *Phys. Rev.* B **64** 020102
[36] Fox A M 2001 *Optical Properties of Solids* (New York: Oxford University Press) p 54
[37] Wan X M, Xu H Q, He T H, Lin D and Luo H S 2003 *J. Appl. Phys.* **93** 4766
[38] Wan X M, Wang J, Chan W L H, Luo H S and Yin Z W 2004 *J. Cryst. Growth* **263** 251
[39] Tauc J C 1972 *Optical Properties of Solids* (Amsterdam: North-Holland) p 372
[40] Wan X M, Luo H S, Wang J and Chan W L H 2004 *Solid State Commun.* **129** 401
[41] Wang Y 2006 *Phys. Rev.* B **73** 014113
[42] Qu W, Zhao X and Tan X 2007 *J. Appl. Phys.* **102** 084101